ECOGRAPHY

Research article

Global variation in ecoregion flammability thresholds

Todd M. Ellis, David M. J. S. Bowman and Grant J. Williamson

School of Natural Sciences, University of Tasmania, Sandy Bay, Australia

Correspondence: Todd M. Ellis (toddellis.wa@gmail.com)

Ecography
2024: e07127
doi: 10.1111/ecog.07127
Subject Editor: Erica Fleishman
Editor-in-Chief: Miguel Araújo
Accepted 7 March 2024

Anthropogenic climate change is altering the state of worldwide fire regimes, including by increasing the number of days per year when vegetation is dry enough to burn. Indices representing the percent moisture content of dead fine fuels as derived from meteorological data have been used to assess geographic patterns and temporal trends in vegetation flammability. To date, this approach has assumed a single flammability threshold, typically between 8 and 12%, controlling fire potential regardless of the vegetation type or climate domain. Here we use remotely sensed burnt area products and a common fire weather index calculated from global meteorological reanalysis data to identify and describe geographic variation in fuel moisture as a flammability threshold. This geospatial analysis identified a wide range of flammability thresholds associated with fire activity across 772 ecoregions, often well above or below the commonly used range of values. Many boreal and temperate forests, for example, can ignite and sustain wildfires with higher estimated fuel moisture than previously identified; Mediterranean forests, in contrast, tend to sustain fires with consistently low estimated fuel moisture. Statistical modelling showed that flammability thresholds derived from burnt area are primarily driven by climatological variables, particularly precipitation and temperature. Our analysis also identified complex associations between vegetation structure, fuel types, and climatic conditions highlighting the complexity in vegetation–climate–fire relationships globally. Our study provides a critical, necessary step in understanding and describing global pyrogeography and tracking changes in spatial and temporal fire activity.

Keywords: biogeography, climate change, fire risk, fuel moisture, pyrogeography

Introduction

There is growing consensus that anthropogenic climate change is causing longer and hotter fire seasons (Balch et al. 2022, Ellis et al. 2022, Jain et al. 2022), with a corresponding increase in the number of wildfires spreading rapidly and with adverse social, ecological, and economic impacts (Bowman et al. 2017, Duane et al. 2021). Climate projections suggest this trend is likely to continue throughout the 21st century (Flannigan et al. 2013, Wotton et al. 2017, Abatzoglou et al. 2019, 2021). The

annual area burned in forests in the western United States, for example, has increased rapidly in the last half century (Westerling 2016, Williams et al. 2019) – albeit this trend is partially driven by a long history of land-use practices such as fire suppression and the reduction or loss of Indigenous fire use after colonisation (Abatzoglou et al. 2018). Current climatological and ecological modelling suggests the occurrence of severe fire events in the USA recently exhibited by the widespread ecological damage in the 2020 fire season (Higuera and Abatzoglou 2020, Abatzoglou et al. 2021) will continue to increase across affected regions due to anthropogenic climate change (Bowman et al. 2020). The potential severity of these events, however, may be reduced by fuel management intervention such as the promotion of regular low-severity fire that restores pre-colonial fire regimes to western North American forests (Abatzoglou et al. 2021, Hessburg et al. 2021). A similar increase in severe fires is also evident in southeastern Australia (Sharples et al. 2016, Abram et al. 2021), where trends in both drought and extreme fire weather combined with the loss of Indigenous fire use are believed to have contributed to the high social, economic, and ecological costs of the 2019–2020 fire season, dubbed the Australian Black Summer (Boer et al. 2020, Nolan et al. 2020, Canadell et al. 2021, Collins et al. 2021, van Oldenborgh et al. 2021, Mariani et al. 2022).

To monitor and potentially mitigate these risks, research has identified common wildfire behaviour and ignition determinants that shape fire regimes (Bradstock 2010, Murphy et al. 2013). Dead fine fuel moisture content (DFFMC) has been identified as a key determinant of the spread of vegetation fire. The moisture content of dead surface vegetation such as leaves, bark, twigs, and grass is capable of equilibrating with atmospheric humidity in under 10 h, and consequently represents the most ignitable component of vegetation. As the ignition of these fuels can then provide the energy to ignite both larger dead fuel components and live fuels, DFFMC is a key determinant of overall wildfire occurrence, behaviour, and greater pyrogeographic patterns. DFFMC can be measured directly in the field (Bowman et al. 2020) or estimated using meteorological indices such as vapour pressure deficit or the Canadian Forest Fire Weather Index (FWI) System (van Wagner 1987). Accordingly, derived or measured DFFMC functions as a prominent proxy for the potential of surface litter to ignite and sustain wildfire spread (Murphy et al. 2013, Flannigan et al. 2016, Kelley et al. 2019). DFFMC is also of fundamental importance in shaping spatial and temporal patterns of landscape fires from local to global scales. For example, moisture differences control the conditions for rapid fire spread across different vegetation types such as savannas and rainforests (Little et al. 2012).

Prior research identified values of DFFMC associated with the upper and lower bounds of wildfire potential (Fernandes et al. 2008, Wotton 2008, Slijepcevic et al. 2015, Flannigan et al. 2016, Nolan et al. 2016, Boer et al. 2017, Filkov et al. 2019, Clarke et al. 2022). For instance, FWI- or vapour pressure deficit-derived DFFMC values between 8 and 12% have been linked to wildfires that evade suppression efforts (Slijepcevic et al. 2015, Flannigan et al. 2016, Nolan et al. 2016, Boer et al. 2017, Filkov et al. 2019). Values of up to 30% have been found to represent the upper limits for sustained fire spread in vegetation (Fernandes et al. 2008) under current atmospheric oxygen concentrations due to carbon fibre saturation (Luke and McArthur 1978, Scott and Glasspool 2006).

Global and regional studies frequently estimate DFFMC within the FWI System due to its ease of calculation and interpretation (Field 2020); these studies have often applied single-value thresholds to assess patterns and likely trends in global fire potential. For instance, an established 10% threshold (Wotton 2008, Flannigan et al. 2016) was used to infer that the proportion of fire seasons falling below this critical threshold had significantly increased between 1979 and 2019 for most ecoregions worldwide (Ellis et al. 2022). Such a shift is likely to affect established fire regimes, particularly in more productive or wet ecoregions.

There are, however, inherent problems with applying single-value thresholds to compare different vegetation types and climate domains. Ecoregions have evolved with fire differently in response to naturally occurring environmental and biological constraints like soil fertility, climate, and the local biota. These evolutionary divergences have led, for example, to differences in leaf flammability among species caused by physiological traits or leaf chemistry (Mutch 1970, Bowman et al. 2014a, Varner et al. 2015). Additionally, it is well understood that drivers of fire regimes can differ based on the local vegetation structure and the dominant fuel types – many of which have been heavily reshaped by anthropogenic factors (e.g. rural population growth and promotion of invasive plant species: Pausas and Keeley 2021). It is thus unlikely that a single DFFMC value could reflect the ignitability in both Mediterranean and tropical forests, for example, where fire spread is limited by fuel availability or dry conditions, respectively. Additionally, it is unclear if different values of DFFMC are associated with specific fire behaviour – for example, low thresholds causing crown fires and high thresholds associated with surface fires. Furthermore, fire danger indices were developed for specific, regional forest types. The FWI System was developed based on mature *Pinus banksiana* and *P. contorta* landscapes in southern Canada (van Wagner 1987, Wotton 2008). Despite the FWI System's established global applicability, it was never assumed that the vegetation in these forests is globally representative, and use of the FWI System may consequently be inappropriate for assessing fire potential or fuel moisture in different vegetation types (Aguado et al. 2007, Wotton and Beverly 2007, Schunk et al. 2017). This raises a question about how a given fire weather index can best be used to retain local relevance by identifying ecoregion-specific thresholds below which fire spread is likely to be uncontrollable (Clarke et al. 2022).

Building on these studies, we sought to answer the question of whether a universal fuel moisture threshold exists as a control on fire ignition and spread, while advancing our understanding of how fuel moisture acts as a switch for landscape fire both regionally and globally. Using a comprehensive dataset of over 700 hierarchically defined ecoregions, we

identified flammability thresholds as the DFFMC value most strongly associated with rapid step changes in remotely sensed burnt area records for each ecoregion. Our methods (Fig. 1) bypassed the issues inherent with applying the FWI System globally by localising the relationship between DFFMC and fire to each ecoregion with associated satellite burnt area records. For these same ecoregions, we then applied nonmetric multidimensional scaling to a suite of climatic variables with well-established links to fire. We visualised the variable reduction from this scaling to inform our development of an inferential statistical model and to verify the veracity of flammability thresholds as a biophysical, localised mechanism with both Bayesian effects probability measures and measures of variable importance. This combination of exploratory analysis and modelling provided a channel to examine both the biogeographic and climate characteristics shaping our identified flammability thresholds as constraints on fire ignition and spread, and ensured they represent a biophysical reality.

Material and methods

Geospatial classification

We used the Terrestrial Ecosystems of the World regional classification system hosted by the World Wildlife Fund

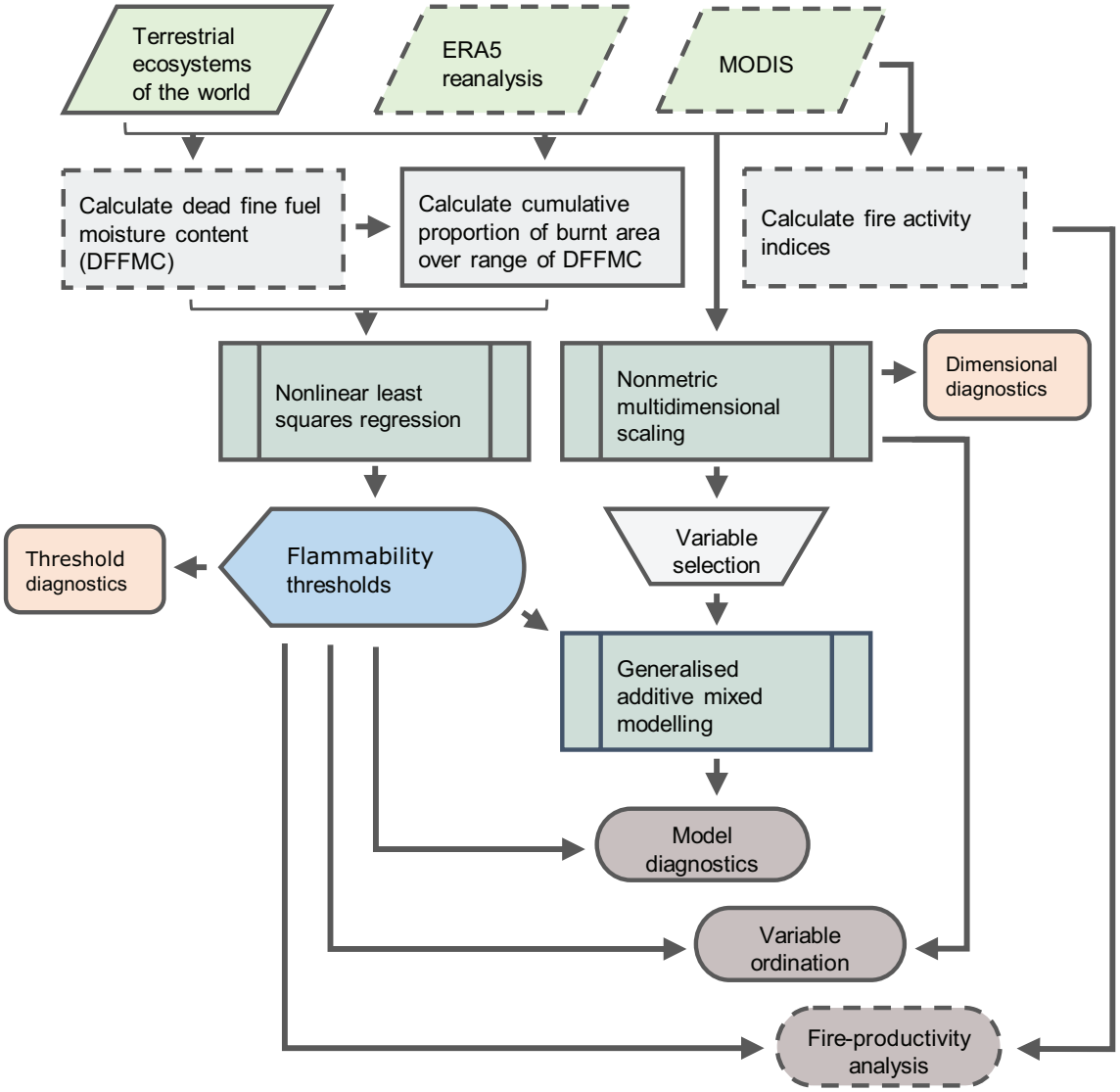

Figure 1. Data sources, methods, and outputs. Dashed outlines represent 0.25° gridded data or analyses performed at the 0.25° grid cell level. Solid outlines represent data or analyses summarised at the ecoregion level. ERA5 reanalysis data included daily meteorological time-series (Hersbach et al. 2020) and bioclimatic indicator means (BIO01, BIO12 and BIO15: Wouters et al. 2021). MODIS products included MCD64CMQ (Giglio et al. 2018), MOD17A3 (Running et al. 2015), MOD44B (DiMiceli et al. 2015), and MCD14DL (Giglio et al. 2003). Output products were flammability threshold diagnostics (e.g. two-way Dunn's test for pairwise multiple comparisons), model diagnostics (Table 1 and Supporting information), visualised nonmetric multidimensional scaling variable ordination and associated dimensional diagnostics, and the analysis of fire activity indices and net primary productivity.

(Olson et al. 2001, Supporting information). This system groups regions into a hierarchy: eight realms (e.g. the Indo-Malay Archipelago and associated lands in Southeast Asia), 14 biomes (e.g. temperate broadleaf and mixed forests), and 867 ecoregions (e.g. Madagascar's subhumid forest). These ecoregions represent distinct biota, but do not represent the real effects of human land-use practices such as agricultural clearing. We removed 95 of the 867 original ecoregions from our analyses, including 76 ecoregions with no associated fire records (e.g. those in Antarctica). In addition, we removed the mangroves biome from all analyses, as this biome comprises only 19 small, discontinuous ecoregions with fire histories primarily determined by neighbouring ecoregions.

Identifying and assessing the ecoregion flammability threshold

We used estimated DFFMC (%) as drawn from the FWI System's fine fuel moisture code (van Wagner 1987) as a foundation for identifying ecoregional flammability thresholds. We chose this estimation of DFFMC due to its established global applicability and ease of both calculation and interpretation (Wotton 2008, Field 2020). To calculate DFFMC, we used the European Centre for Medium-Range Weather Forecast's ERA5 atmospheric reanalysis data (Hersbach et al. 2020) due to its accessibility and worldwide coverage. We used these data to calculate daily DFFMC representing noon local standard time from 1979 through 2019 at a gridded 0.25° spatial resolution. High latitude overwintering periods were removed from the records to reduce the false identification of dry winter periods as highly flammable (McElhinny et al. 2020) (see Fig. 1 for a detailed workflow diagram).

To identify the flammability threshold associated with fire ignition and spread in each ecoregion, we first calculated the cumulative proportion of burnt area from the Moderate Resolution Imaging Spectroradiometer (MODIS) MCD64CMQ product (2001–2021: Giglio et al. 2018) over the full range of potential thresholds by ecoregion. We chose burnt area from available MODIS data due to the biophysical constraint of fuel moisture on fire spread and thus wildfire potential (Slijepcevic et al. 2015). Other measures may be more obfuscated by anthropogenic factors (e.g. ignitions: Balch et al. 2017) or weather (e.g. fire radiative power: Hernandez et al. 2015). We constrained the upper bounds of potential thresholds to 70% DFFMC to allow for a degree of uncertainty well above the known limits of the fibre saturation point (Fernandes et al. 2008). We summarised ecoregional DFFMC records to match the temporal resolution of the burnt area record (2001–2019) by extracting the 25th percentile from each month's distribution of daily, grid cell-level DFFMC records. For each month in the shared record, this equation assumes the 25th percentile of the ecoregion's daily DFFMC distribution reflects that ecoregion's driest period. We then used nonlinear least squares regression to fit a logistic curve to the relationship between the cumulative proportion of burnt area (BA) and the upper limit of each ecoregion's driest monthly DFFMC quartiles:

$$\mathrm{P(BA < DFFMC)} = \frac{\phi_1}{1 + e^{\frac{-(\phi_2 - \mathrm{DFFMC})}{\phi_3}}}, \quad (1)$$

where ϕ_1, ϕ_2 and ϕ_3 are the asymptote, curve inflection point, and scale parameter of the curve, respectively. We extracted ϕ_2 as the inflection point with the greatest marginal increase in the cumulative proportion of burnt area for a given reduction in DFFMC. The DFFMC value at ϕ_2 is the threshold constraining flammability for a given ecoregion. We also extracted the reciprocal of ϕ_3 as an estimate of the inflection point slope and a proxy for the associated threshold strength. Fire data within the DFFMC constraints were insufficient to identify a flammability threshold for 74 ecoregions. Instead of removing these ecoregions from our analyses, we imputed the missing values as the median threshold from the same hierarchical realm and biome classifications where available. For example, the 74 ecoregions include three boreal forest ecoregions in the Nearctic and Palearctic realms. We imputed the median flammability threshold for Nearctic boreal forests (14%) as the value for the two Nearctic ecoregions, and the median threshold for Palearctic boreal forests (16.3%) as the value for the Palearctic ecoregion. See Supporting information for all modelled ecoregional P(BA < DFFMC) curves and biome-level means.

We assessed the identified flammability thresholds by first visualizing threshold distributions by biome, highlighting the median and quantile-based intervals. We confirmed the apparent effects of median biome differences with a Kruskal–Wallis rank sum test (Kruskal and Wallis 1952), and then identified the mean rank differences between biomes with a two-way Dunn's test for pairwise multiple comparisons (Dunn 1961). We extracted non-significant differences between biomes, highlighting the similarities in fuel–fire relationships.

Statistical analyses

To identify the climatological factors driving burnt area-derived flammability thresholds, we used nonmetric multidimensional scaling and generalised additive mixed modelling. First, we applied the ordination to a suite of climatological and ecological data with known associations with wildfire ignition or spread, and then plotted the ordination against our identified thresholds. We used bioclimatic indicator means (1979–2018) for annual precipitation (BIO12: m), annual temperature (BIO01: K), and precipitation seasonality (BIO15: %) from the ERA5 reanalysis data, which are available via the Copernicus Climate Data Store (Hersbach et al. 2020, Wouters et al. 2021). We also used three additional MODIS products: mean annual net primary productivity (NPP: t C ha^{-1} $year^{-1}$) calculated from 2000 through 2015 (MOD17A3: Running et al. 2015) and the median percentage of an ecoregion represented by herbaceous and tree cover in 2020 (MOD44B: DiMiceli et al. 2015). We tested both two- and three-dimensional ordination on the basis of exploratory stress scree and Shepard plotting, ultimately choosing the two-dimensional ordination with a stress index of 0.125

for simplicity (Supporting information). We plotted the new, reduced dimensions with scatterplot variable ordination with the underlying distribution of flammability thresholds to explore the effects of the different climatological variables and reduce the number of variables retained in the model.

Building on the previously identified association between intermediate NPP and fire activity (Pausas and Bradstock 2007, Krawchuk and Moritz 2011, Pausas and Ribeiro 2013, Bowman et al. 2014b, Ellis et al. 2022), we plotted mean fire activity as a function of global NPP underlain by our identified flammability thresholds and the associated threshold strength. This analysis uses 0.25° ERA5 grid cells for NPP and indexed fire activity (Ellis et al. 2022). Following those prior analyses, we calculated fire activity indices (Pausas and Ribeiro 2013) with the mean annual (2002–2020) number of fire detections recorded in the MODIS active fire database (MCD14DL: Giglio et al. 2003) while excluding permanent, anthropogenic heat sources. This combination provides insight into how flammability (via thresholds and the associated strength) is shaped by global patterns of NPP and indexed fire activity.

To measure the effects of climatological variables on flammability thresholds, we employed generalised additive mixed modelling with a Bayesian framework. Our model was not intended to make predictions but to evaluate whether the identified thresholds were a functioning, biophysical mechanism on ecoregion-level fire behaviour ultimately shaped by moisture availability. Because our flammability thresholds can be interpreted as a percentage with a strong positive skew, we estimated the response likelihood function on a beta distribution. Although DFFMC as derived from the FWI System can reach 250%, our thresholds all fall under 100% due to the 70% constraint we applied. It is unlikely that any potential flammability threshold is above 70% given vegetation's theoretical maximum fibre saturation point of 30% (Fernandes et al. 2008). Informed by our exploratory analysis of the thresholds and the variable ordination, we retained precipitation, temperature, precipitation seasonality, and herbaceous vegetation cover as fixed continuous effects in the model. Of the highly colinear variables, we chose annual precipitation over both NPP and percent tree cover due to the former's reliance on precipitation, and the latter's link to herbaceous cover. As realm and biome type do not reflect true vegetation, we retained both as interactive random effects. See the Supporting information for additional model development details, including data preparation steps and specific model parameters.

To evaluate and explain our model, we focused on variable importance via permuted root-mean-square error (RMSE) dropout loss and Bayesian effects probability measures. These two approaches provide simple measures of the effects our modelled climate variables have on the global distribution of flammability thresholds. We calculated the influence of individual variables in the model with sampled (n = 1,000) change in the RMSE loss function over 100 permutations. We then evaluated the continuous fixed effects of our model with sequential effect existence and significance testing. This method describes the effects of model parameters, providing three probabilities of overall effect direction (i.e. existence), practical effect significance, and size (i.e. strength) while also being easy to interpret due to their rough equivalence to statistical significance (e.g. $p < 0.05$ or a probability greater than 95%).

Results

Distributions of ecoregion flammability thresholds

We identified flammability thresholds for 772 of 867 ecoregions classified in the Terrestrial Ecosystems of the World dataset (Olson et al. 2001), representing 95% of the total classified area (135.2 M km^2: Fig. 2a and 3). The global mean flammability threshold was 12.2%, with a median of 11.5% and an interquartile range of 6.92%. Thresholds in 17 ecoregions (0.8 M km^2) were above the expected maximum of 30%; most of these thresholds were likely due to fuel moisture playing a smaller role in fire or insufficient fire data. The strongest relationships between DFFMC and burnt area appeared to be in deserts, tropical and subtropical savannas, higher-latitude forests, and some tundra environments (Fig. 2b).

Across biomes, the lowest identified flammability thresholds were associated with shrublands, woodlands, and savannas (Fig. 3). The highest identified thresholds tended to be associated with higher-latitude forests and tundra. Wetter temperate and tropical forested biomes were most like these high-latitude biomes, but also tended to have the widest range of thresholds, suggesting more complex relationships among fire, fuel moisture, and human activity. The Kruskal–Wallis rank sum test for differences in flammability thresholds between biomes was significant ($p < 0.001$), while the pairwise multiple comparisons calculated with Dunn's test highlighted similar and dissimilar biomes. The statistical grouping of biomes with similar flammability thresholds showed a clear gradient across climate, NPP, and vegetation types, albeit with a wide intra-biome variability associated with the complexity of ecoregions within biomes (Fig. 3). See the Supporting information for pairwise multiple comparison statistics and summary statistics for flammability thresholds.

Climatic controls on flammability thresholds

The first dimension of the two-dimensional nonmetric multidimensional scaling was primarily driven by precipitation and associated proxies: higher annual precipitation, NPP, and more tree cover were linked, influencing fuel–fire relationships in ecoregions where fire is historically limited by fuel moisture (Kelley et al. 2019, Fig. 4a–b). The second scaled dimension was driven primarily and negatively by temperature and was strongly linked to biomes such as deserts where fire is historically limited by fuel availability. Higher herbaceous vegetation cover was also prominent on the second dimensional axis, and was associated with cooler, drier ecoregions such as tundra. Precipitation seasonality had a negative effect across the first and second scaled dimensions, with higher values of precipitation seasonality representing stronger seasonal dryness (e.g. savannas with arid summers).

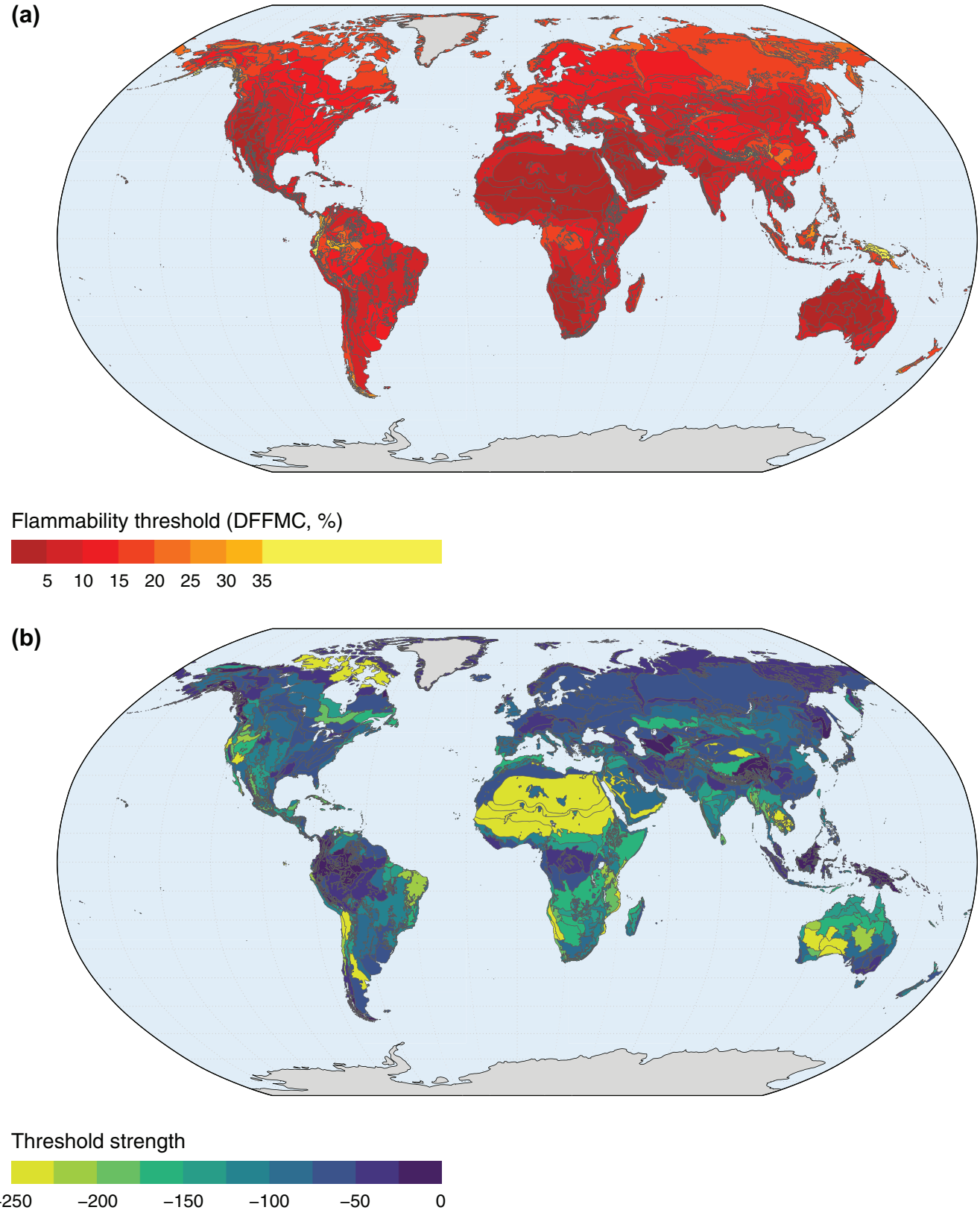

Figure 2. Global distributions of (a) identified ecoregional flammability thresholds and (b) the associated threshold strength extracted from the P(BA < DFFMC) models. All flammability thresholds above 35% were binned into a single grouping. Lower values of threshold strength represent stronger associations between cumulative burnt area probability and DFFMC. Imputed values are included. DFFMC, dead fine fuel moisture content.

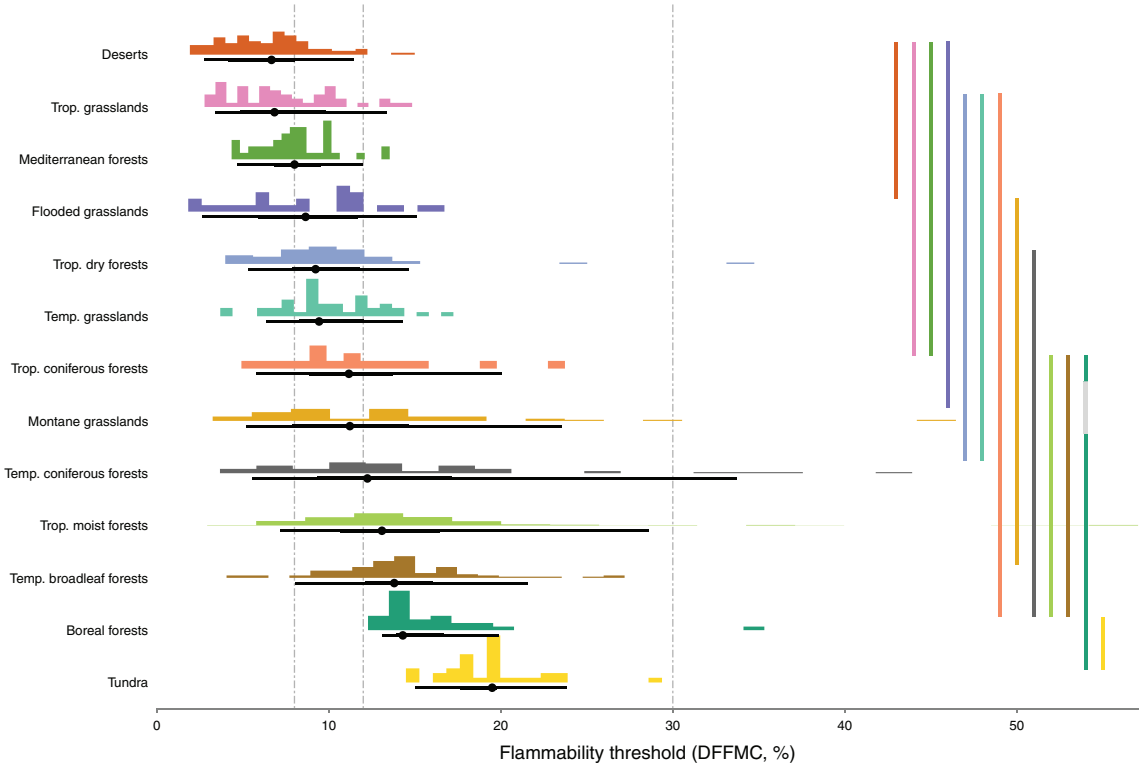

Figure 3. Distribution of the flammability thresholds by biome type, ordered by median flammability threshold. Point and line intervals under histograms represent the median equal-tailed distribution intervals of 50 and 90%. Dashed vertical lines reference threshold values (8, 12, and 30%) identified as biophysical thresholds constraining fire ignition and spread in prior research (Fernandes et al. 2008, Wotton 2008, Flannigan et al. 2016, Nolan et al. 2016, Boer et al. 2017, Filkov et al. 2019). See the Supporting information for underlying dead fine fuel moisture content (DFFMC) distributions used to identify flammability thresholds. Vertical lines on the right reflect non-significant differences in Dunn's Z statistics for pairwise multiple comparisons. For example, the mean rank of flammability thresholds for deserts is comparable to the three biome types below it. The value associated with boreal forests was significantly different from that associated with montane grasslands, but not tropical coniferous forests.

The average flammability threshold was well below the expected 30% limit for carbon fibre saturation across the range of calculated fire activity indices and NPP (Fig. 5a). NPP is below 10 t C ha^{-1} $year^{-1}$ in most of Earth's ecoregions by land area (Fig. 5a). Within the intermediate NPP range (roughly 1.2–5.4 t C ha^{-1} $year^{-1}$) where fire activity indices are maximal, thresholds were moderately higher. The lowest flammability thresholds occurred within the least productive environments. Low thresholds also occurred with higher NPP in ecoregions that frequently burn (e.g. annually burnt tropical grasslands). Both areas of extremely low thresholds tended to have the most extreme threshold strength (Fig. 5c).

Our generalized additive model of flammability thresholds yielded an R^2 of 0.682 and an RMSE of 0.038. See the Supporting information for comparable statistics for training, testing, and cross-validation datasets. The highest probabilities of effect existence for the three non-linear bioclimatic variables were 100% (annual precipitation), 99.9% (precipitation seasonality), and 98.8% (annual temperature). The probability of existence of the linear percent herbaceous cover effect was 93.3%. Probabilities of effect significance and size were similar, with only herbaceous cover below 95% (Table 1). Mean annual precipitation, mean annual temperature, and mean precipitation seasonality had the greatest influence on the model's accuracy, followed by the terrestrial realm and biome classifications as random effects. Median percent herbaceous cover had a consistent, negligible effect on the model RMSE loss. Additionally, all predictor variables except annual precipitation were negatively associated with flammability thresholds. See the Supporting information for model evaluation steps, including conditional effects and posterior distributions.

Discussion

The significant variability in the biogeography of flammability thresholds we revealed (Fig. 2a, 3) suggests that a generalised, universal fuel moisture threshold does not capture differences in flammability among vegetation types. This variability is explained by climatological variables such as precipitation and temperature, which in turn influence the distribution of vegetation. Climate needs to be considered in concert with the threshold strength and fire activity, as outlined below. These considerations are important in understanding global pyrogeography, including the likely effects of climate change on fire regimes, and ecoregions and biomes where fire activity is increasing.

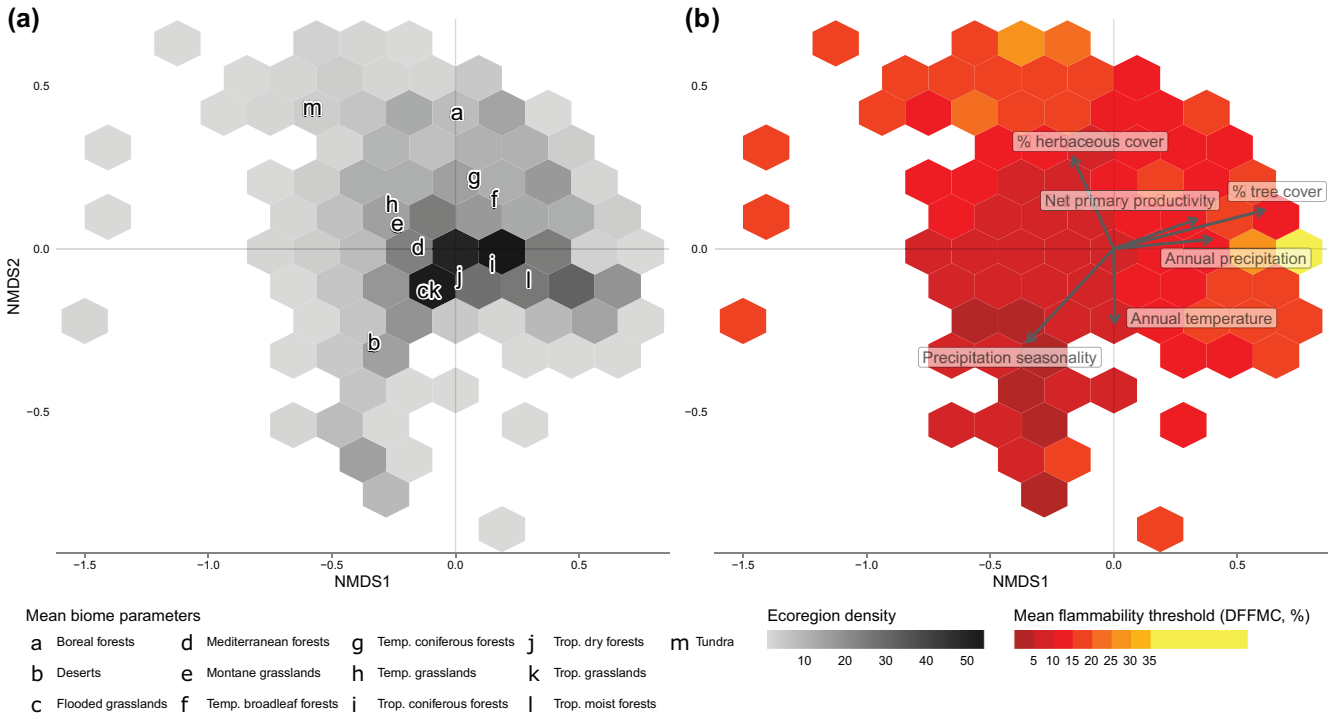

Figure 4. Site scores for the first and second dimensions produced by nonmetric multidimensional scaling (NMDS1 and NMDS2) of climatological variables for which associations with wildfire ignition or spread are well-established. (a) Density distribution of the ecoregions included in the analyses. Points represent the biome-level mean site scores for both dimensions. (b) Median underlying flammability threshold. Arrows represent the NMDS species scores, or strength and direction of variable influence within the new scaled dimensions.

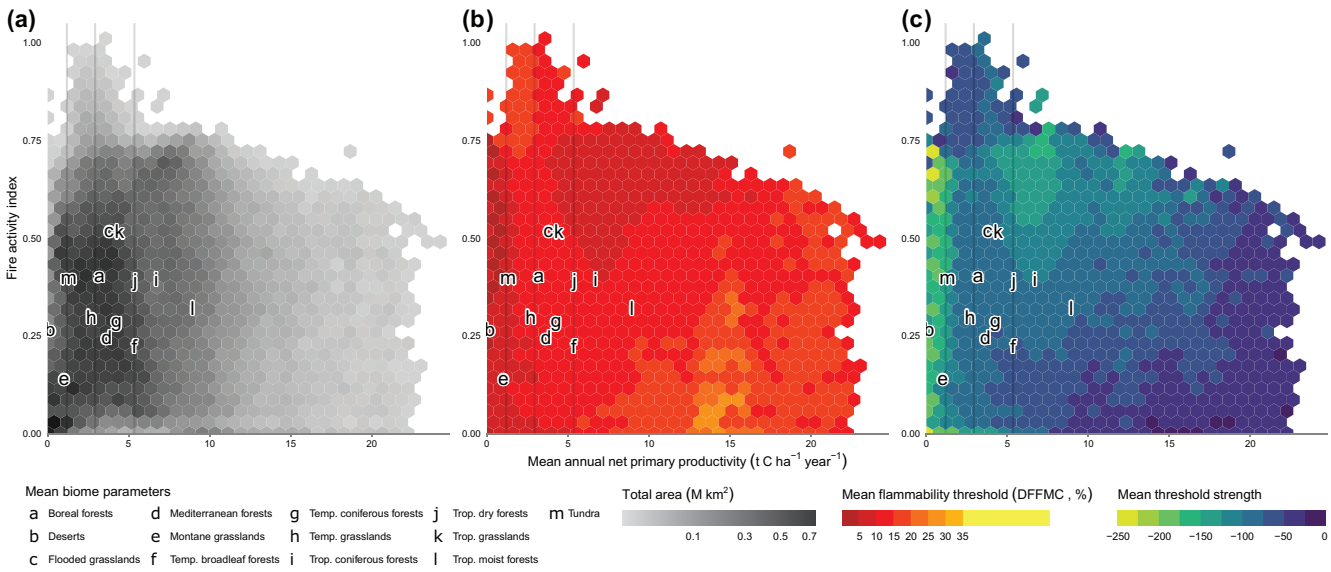

Figure 5. Adaptation of the intermediate productivity–fire activity hypothesis as drawn from Ellis et al. (2022) with (a) the total area (M km^2) of Earth's surface represented, (b) the mean underlying ecoregional flammability threshold, and (c) the mean underlying threshold strength. Solid vertical lines in all figures highlight the 25th, 50th, and 75th percentiles of global net primary productivity (NPP), roughly illustrating the range of intermediate NPP most strongly associated with fire activity (~ 1.2–5.4 t C ha^{-1} year^{-1}); points represent the mean locations of biome-level NPP and fire activity indices.

Table 1. Continuous linear and non-linear model parameters. The median and 89% highest density interval (HDI) both reflect the posterior predictive distribution. Effect existence, effect significance, and effect size are probabilities. Effect significance was based on an estimated region of practical equivalence (ROPE) value of 0.181 and the size estimate was based on a default recommended value of 0.3 following exploratory analysis.

Parameter	Parameter type	Median	89% HDI	Existence	Significance	Size
Mean annual precipitation	Non-linear (k = 5)	3.451	[2.294, 4.575]	100.0%	100.0%	100.0%
Mean precipitation seasonality	Non-linear (k = 8)	−1.337	[−2.183, −0.669]	99.9%	99.7%	99.4%
Mean annual temperature	Non-linear (k = 5)	1.176	[0.400, 1.922]	98.8%	97.3%	96.1%
Median % herbaceous cover	Linear	−0.126	[−0.259, 0.006]	93.3%	26.0%	1.9%

The biogeography of flammability thresholds

The global averages of our flammability thresholds are close to the previous extreme values of 8–12% (Wotton 2008, Slijepcevic et al. 2015, Flannigan et al. 2016, Nolan et al. 2016, Boer et al. 2017, Filkov et al. 2019, Ellis et al. 2022). This suggests that commonly used thresholds derived from the FWI System and ERA5 reanalysis data reflect biophysical factors controlling fire ignition and spread in many ecosystems. Despite this, relying on a global average oversimplifies local relationships between fuel moisture and fire, and ignores variation in the fibre saturation point among landscapes and vegetation types (Fernandes et al. 2008, Alvarado et al. 2020). A generalised threshold will often under- or over-estimate an ecoregion's flammability threshold, with the threshold across nearly 70% of Earth's surface above 12% or below 8%. The geographic distribution of thresholds (Fig. 2a) and differences between and within biomes (Fig. 3) highlight where this oversimplification does not reflect the ecoregional flammability threshold. This includes, for instance, boreal forest (Q1: 13.9%, Q3: 16.6%) and tundra (Q1: 17.7%, Q3: 19.8%) ecoregions, and North American *P. banksiana* and *P. contorta* forests where the FWI system originated (van Wagner 1987). In such high-latitude ecoregions, the general threshold likely misrepresents the true fuel moisture content associated with burnt area (Fig. 3). When applying these general thresholds for trend analysis or forecasting within these ecoregions, fire danger may be underestimated (Ellis et al. 2022).

Biogeographically variable flammability thresholds are needed given the role water availability – including the moisture content of both live and dead fuels – plays in fuel accumulation (Murphy et al. 2013). A universal threshold oversimplifies how plants in different ecoregions may have co-evolved with fire. A bespoke threshold likely can more accurately capture the variation in live and dead fuel moisture content associated with the phylogeographic effects of foliage flammability (Bowman et al. 2014a) and the structure of vegetation and fuel (Pausas and Keeley 2009, Keeley et al. 2011, Alvarado et al. 2020). For example, accumulation and continuity of fuel is necessary to sustain a wildfire ignition in many ecoregions. The availability and type of fuel in these ecoregions depends on the local climate. Tundra and deserts rarely have enough fuel to burn regardless of whether the surface litter is below the flammability threshold. Similarly, fuel growth in many temperate coniferous forests has a years- to decades-long lag typical of the negative exponential fuel accumulation curve (Olson 1963). The most productive tropical forests, by contrast, tend to retain enough water that wildfires are rare (Murphy et al. 2013). In these more productive ecoregions, the threshold more accurately reflects the flammability threshold if the threshold strength is also highly negative. In seasonally dry ecoregions, fuel moisture determines whether vegetation can ignite and maintain a wildfire, albeit it is likely that variation in foliar flammability also contributes to flammability threshold variance in comparable climates (e.g. *Eucalyptus* versus *Pseudopanax*: Wyse et al. 2016).

Interpreting regional variability in flammability thresholds

Because we applied methods to derive flammability thresholds to global data, our results reflect an ecological generalisation. Although there is variability within each ecoregion due to terrain, vegetation, and fuel structure, flammability thresholds are still biologically meaningful and should be interpreted as representative. That is, an average DFFMC near or below our identified threshold for a given ecoregion is not representative of the moisture content of all fuel particles. The flammability of dead fine fuels differs among species and over landscapes where species co-occur (Varner et al. 2015), albeit some thresholds are still inaccurate or imprecise. Sources of error include the short length of the remotely sensed burnt area records and the difference in importance of fuel moisture as a fire trigger across the NPP gradient (Fig. 5a–c). For instance, in some ecoregions, the modelled P(BA < DFFMC) relationships for some ecoregions include gradual shifts in the cumulative proportion of burnt area over the full range of DFFMC (Supporting information). In other cases, we identified thresholds well above the upper limits of the fibre saturation point (i.e. > 30%: Fernandes et al. 2008). Both of these cases could reflect a lack of fire data within the ecoregion, differences in local land use (e.g. uncultivated savanna or agriculture: Le Page et al. 2010, Andela et al. 2017), a limited role of fuel moisture in fire ignition and spread in that ecoregion (Alvarado et al. 2020), or a combination of these factors. Our use of the 25th percentile of each month's daily DFFMC records to identify the flammability threshold also constrains the possible thresholds identified by controlling the range of available DFFMC.

The biases in the ERA5 reanalysis product also mean the accuracy of our identified thresholds reflecting true moisture content will be lower within the tropics (Lavers et al. 2022), and that some of the variability in the tropics is independent of the biophysical variation expected among true flammability thresholds. Burnt area is unable to capture

different causes or kinds of fire and fire behaviour, and some burnt area-derived flammability thresholds may be impacted by intentional application of fire. Additionally, our use of burnt area means the flammability thresholds will not reflect a ubiquitous relationship between fuel moisture and fire behaviour for every ecoregion. While our thresholds may reflect a critical point for higher fire spread rates for biome types such as boreal forests, they may also reflect low-severity fires typical of, for example, tropical grasslands. Furthermore, the ERA5 resolution (0.25°) may be too coarse to differentiate the climatology of small ecoregions from that of surrounding regions. This includes most flooded grasslands and savanna, and tropical and subtropical coniferous forests given their small size, number, and geographic range (Supporting information).

Our results suggest that climatic factors explain a large proportion of the variation in the burnt area-derived flammability thresholds among the ecoregions (Fig. 4a–b, Table 1 and Supporting information). Overlaying biome means onto the ordination, for example, showed that the lowest thresholds in deserts (Q1: 4.2%, Q3: 8%) are strongly associated with precipitation seasonality and low values of precipitation variables. The highest thresholds in tundra (Q1: 17.7%, Q3: 19.8%) were associated with high percent herbaceous cover and lower temperatures. Higher-latitude boreal forests (Q1: 13.9%, Q3: 16.6%) and coniferous forests (Q1: 9.3%, Q3: 17.2%) were associated more strongly with a combination of precipitation, temperature, and temperature seasonality. However, the precipitation dimension includes the effects of NPP and percent tree cover, consistent with pyrogeographic theory stating that global fire activity is shaped by productivity (Pausas and Bradstock 2007, Pausas and Ribeiro 2013, Jones et al. 2022). For example, low NPP deserts and xeric shrublands feature the most extreme combination of low flammability thresholds, threshold strength, and NPP on Earth (median of 0.17 t C ha^{-1} $year^{-1}$; Fig. 5b–c). However, the driest of these environments experience little fire activity (< 0.2 indexed fire activity in Fig. 5a–c), and fire is ultimately controlled by intermittent periods of high productivity rather than moisture content (Archibald et al. 2009, Bradstock 2010, Kelley et al. 2019).

We acknowledge that the mechanisms of ecoregional variation remain elusive. For instance, we suspect the predominance of live fuels with flammable foliage in Mediterranean ecosystems may explain why we identified lower fuel moisture thresholds for this biome. These live fuels draw water from deeper soil layers not directly captured in our DFFMC metric and reach the point of ignitability under drought conditions (Dimitrakopoulos and Papaioannou 2001). In many ecoregions, the local climate influences possible flammability thresholds. The colder temperatures and seasonal snowpack in boreal forests, for example, mean that the potential for flammability thresholds to be near or below 12% DFFMC is limited (Supporting information). In contrast, Mediterranean ecosystems' low flammability thresholds reflect drought conditions in regularly warm and dry environments. Additionally, specific local vegetation adaptations and structural differences may be more influential in determining flammability thresholds in some ecoregions. Australian *Eucalyptus* broadleaf forests, for example, have both highly flammable live foliage and dead fine fuels.

The measure of fuel moisture content we used is meteorologically determined and represents an average over large areas. At local scales, multiple fuel types and sizes (e.g. grass, litter, coarse woody debris) are present, and each potentially have different fuel moisture content. Thus, a single DFFMC for a given ecoregion inherently represents different local and fuel-specific moisture values for all live and dead fuels available to burn. Understanding the mechanisms underlying variation in flammability thresholds at finer scales than highlighted here requires research at the fuel-bed and fuel-particle scales (Varner et al. 2015, Jolly and Johnson 2018).

The relationship among fire activity, fuel moisture, and fuel availability invites consideration of climate change, which can manifest directly (via fuel moisture) and indirectly (via production of phytomass). As ecoregions shift from one biome type to another or along the NPP gradient, the associated fire activity, flammability thresholds, and threshold strength can be expected to shift as well. Tropical and subtropical rainforests, for example, feature high moisture availability, fuel loads, and flammability thresholds (Fig. 5a–c). These ecoregions are consequently at risk of ecological state change primarily driven by land-use impacts on fire regimes (Le Page et al. 2010, Canadell et al. 2021) and recent drying trends (Ellis et al. 2022). Mediterranean forests are among the least productive forests in the world (Fig. 5a–c) and could shift towards savanna or grasslands as drying trends continue, amplifying fuel limitation to burning despite warming and drying (Pausas and Paula 2012, Pausas and Bond 2020). In contrast, fire in most desert landscapes is limited by fuel availability (Bradstock 2010, Murphy et al. 2013, Bedia et al. 2015). These areas are unlikely to have fire regimes driven by anthropogenic climate change except along biome transition lines (Archibald et al. 2009, Senande-Rivera et al. 2022) or where moisture is increasing over time (Ellis et al. 2022). At the upper limits of the intermediate fire-productivity zone, higher NPP (> 4.5 t C ha^{-1} $year^{-1}$) and fire activity (> 0.5 indexed fire activity) also contribute to extreme values of flammability thresholds and threshold strength (Fig. 5b–c). This zone includes some of the environments most at risk under climatic change, including many temperate broadleaf and boreal forests susceptible to ecological transformation under drying climate trends (Ellis et al. 2022, Senande-Rivera et al. 2022) and more productive, climate-limited tropical savanna ecoregions (Alvarado et al. 2020).

Management relevance

Our burnt area-derived flammability thresholds reduce the uncertainty in defining fire season onset. Fire season onset is a key pyrogeographic parameter that further defines fire regimes and pyromes. At the continental scale, for example, fire season onsets in Australia's fire-prone tropical and temperate ecoregions are driven by a distinct latitudinal climate gradient (Murphy et al. 2013, Williamson et al. 2016). The

evident trend for fuel moisture in wet *Eucalyptus* forests along this gradient places those ecoregions at risk of ecological transformation due to increasing fire frequency (Bowman et al. 2014b, Furlaud et al. 2021, McColl-Gausden et al. 2022). In environments where wildfire is of management interest, our flammability thresholds can be used to detect the onset of a fire season in real time, which may inform the allocation of forest management and firefighting resources, and allow tracking of the effects of climate change on fire danger in different landscapes.

The identification of changing length, intensity, and extremes of fire seasons with meteorological data has generated evidence of changing global fire risk. Unlike previous analyses that used generalised thresholds or assumed thresholds between 8 and 12%, we identified biogeographic variation in flammability thresholds. Understanding this variation is a prerequisite for defining the bounds of the current fire seasons, analysing trends in changing fire seasons, and identifying environments most at risk of ecological transformation under predicted future fire seasons. Hence, our global data representing 772 ecoregions are a steppingstone for understanding and managing fire regimes at the ecoregion level under continued anthropogenic climate change and evolving land-use practices.

Acknowledgements – The authors would like to thank Dr Piyush Jain of Natural Resources Canada (piyush.jain@canada.ca) for their work in pre-processing the ERA5 reanalysis data for publication in Ellis et al. (2022). Open access publishing facilitated by University of Tasmania, as part of the Wiley – University of Tasmania agreement via the Council of Australian University Librarians.
Funding – This work was supported by the New South Wales Bushfire Risk Management Research Hub and funded by the New South Wales Department of Planning, Industry, and Environment.

Author contributions

Todd M. Ellis: Conceptualization (equal); Data curation (lead); Formal analysis (lead); Investigation (lead); Methodology (lead); Project administration (equal); Visualization (lead); Writing – original draft (lead); Writing – review and editing (equal). **David M. J. S. Bowman**: Conceptualization (equal); Formal analysis (supporting); Funding acquisition (lead); Investigation (supporting); Methodology (supporting); Project administration (equal); Resources (lead); Supervision (supporting); Validation (supporting); Visualization (supporting); Writing – review and editing (equal). **Grant J. Williamson**: Conceptualization (equal); Data curation (supporting); Formal analysis (supporting); Funding acquisition (supporting); Investigation (supporting); Methodology (supporting); Project administration (equal); Resources (supporting); Supervision (lead); Validation (supporting); Visualization (supporting); Writing – review and editing (equal).

Transparent peer review

The peer review history for this article is available at https://publons.com/publon/10.1111/ecog.07127.

Data availability statement

The flammability thresholds and associated threshold strength estimates developed as part of this project are freely available from the University of Tasmania Research Data Portal: https://doi.org/10.25959/rbk3-5d65 (Ellis et al. 2023).

Supporting information

The Supporting information associated with this article is available with the online version.

References

Abatzoglou, J. T., Williams, A. P., Boschetti, L., Zubkova, M. and Kolden, C. A. 2018. Global patterns of interannual climate–fire relationships. – Global Change Biol. 24: 5164–5175.

Abatzoglou, J. T., Williams, A. P. and Barbero, R. 2019. Global emergence of anthropogenic climate change in fire weather indices. – Geophys. Res. Lett. 46: 326–336.

Abatzoglou, J. T., Battisti, D. S., Williams, A. P., Hansen, W. D., Harvey, B. J. and Kolden, C. A. 2021. Projected increases in western US forest fire despite growing fuel constraints. – Commun. Earth Environ. 2: 227.

Abram, N. J., Henley, B. J., Gupta, A. S., Lippmann, T. J. R., Clarke, H., Dowdy, A. J., Sharples, J. J., Nolan, R. H., Zhang, T., Wooster, M. J., Wurtzel, J. B., Meissner, K. J., Pitman, A. J., Ukkola, A. M., Murphy, B. P., Tapper, N. J. and Boer, M. M. 2021. Connections of climate change and variability to large and extreme forest fires in southeast Australia. – Commun. Earth Environ. 2: 8.

Aguado, I., Chuvieco, E., Borén, R. and Nieto, H. 2007. Estimation of dead fuel moisture content from meteorological data in Mediterranean areas. Applications in fire danger assessment. – Int. J. Wildland Fire 16: 390.

Alvarado, S. T., Andela, N., Silva, T. S. and Archibald, S. 2020. Thresholds of fire response to moisture and fuel load differ between tropical savannas and grasslands across continents. – Global Ecol. Biogeogr. 29: 331–344.

Andela, N., Morton, D. C., Giglio, L., Chen, Y., Van Der Werf, G. R., Kasibhatla, P. S., Defries, R. S., Collatz, G. J., Hantson, S., Kloster, S., Bachelet, D., Forrest, M., Lasslop, G., Li, F., Mangeon, S., Melton, J. R., Yue, C. and Randerson, J. T. 2017. A human-driven decline in global burned area. – Science 356: 1356–1362.

Archibald, S., Roy, D. P., van Wilgen, B. W. and Scholes, R. J. 2009. What limits fire? An examination of drivers of burnt area in Southern Africa. – Global Change Biol. 15: 613–630.

Balch, J. K., Bradley, B. A., Abatzoglou, J. T., Nagy, R. C., Fusco, E. J. and Mahood, A. L. 2017. Human-started wildfires expand the fire niche across the United States. – Proc. Natl Acad. Sci. USA 114: 2946–2951.

Balch, J. K., Abatzoglou, J. T., Joseph, M. B., Koontz, M. J., Mahood, A. L., McGlinchy, J., Cattau, M. E. and Williams, A. P. 2022. Warming weakens the night-time barrier to global fire. – Nature 602: 442–448.

Bedia, J., Herrera, S., Gutiérrez, J. M., Benali, A., Brands, S., Mota, B. and Moreno, J. M. 2015. Global patterns in the sensitivity of burned area to fire-weather: implications for climate change. – Agric. For. Meteorol. 214–215: 369–379.

Boer, M. M., Nolan, R. H., Dios, V. R., Clarke, H., Price, O. F. and Bradstock, R. A. 2017. Changing weather extremes call for

early warning of potential for catastrophic fire. – Earth's Future 5: 1196–1202.
Boer, M. M., de Dios, V. R. and Bradstock, R. A. 2020. Unprecedented burn area of Australian mega forest fires. Nat. Clim. Chang. 10: 171–172.
Bowman, D. M., French, B. J. and Prior, L. D. 2014a. Have plants evolved to self-immolate? – Front. Plant Sci. 5: 590.
Bowman, D. M., Murphy, B. P., Williamson, G. J. and Cochrane, M. A. 2014b. Pyrogeographic models, feedbacks and the future of global fire regimes. – Global Ecol. Biogeogr. 23: 821–824.
Bowman, D. M., Williamson, G. J., Abatzoglou, J. T., Kolden, C. A., Cochrane, M. A. and Smith, A. M. S. 2017. Human exposure and sensitivity to globally extreme wildfire events. – Nat. Ecol. Evol. 1: 0058.
Bowman, D. M., Kolden, C. A., Abatzoglou, J. T., Johnston, F. H., van der Werf, G. R. and Flannigan, M. 2020. Vegetation fires in the Anthropocene. – Nat. Rev. Earth Environ. 1: 500–515.
Bradstock, R. A. 2010. A biogeographic model of fire regimes in Australia: current and future implications. – Global Ecol. Biogeogr. 19: 145–158.
Canadell, J. G., Meyer, C. P., Cook, G. D., Dowdy, A., Briggs, P. R., Knauer, J., Pepler, A. and Haverd, V. 2021. Multi-decadal increase of forest burned area in Australia is linked to climate change. – Nat. Commun. 12: 6921.
Clarke, H., Nolan, R. H., Dios, V. R., Bradstock, R., Griebel, A., Khanal, S. and Boer, M. M. 2022. Forest fire threatens global carbon sinks and population centres under rising atmospheric water demand. – Nat. Commun. 13: 7161.
Collins, L., Bradstock, R. A., Clarke, H., Clarke, M. F., Nolan, R. H. and Penman, T. D. 2021. The 2019/2020 mega-fires exposed Australian ecosystems to an unprecedented extent of high-severity fire. – Environ. Res. Lett. 16: 044029.
DiMiceli, C., Carroll, M., Sohlberg, R., Kim, D.-H., Kelly, M. and Townshend, J. 2015. MOD44B MODIS/Terra vegetation continuous fields yearly L3 Global 250m SIN Grid V006. – NASA EOSDIS Land, Processes DAAC.
Dimitrakopoulos, A. P. and Papaioannou, K. K. 2001. Flammability assessment of Mediterranean forest fuels. – Fire Technol. 37: 143–152.
Duane, A., Castellnou, M. and Brotons, L. 2021. Towards a comprehensive look at global drivers of novel extreme wildfire events. – Clim. Change 165: 43.
Dunn, O. J. 1961. Multiple comparisons among means. – J. Am. Stat. Assoc. 56: 52–64.
Ellis, T. M., Bowman, D. M. J. S., Jain, P., Flannigan, M. D. and Williamson, G. J. 2022. Global increase in wildfire risk due to climate-driven declines in fuel moisture. – Global Change Biol. 28: 1544–1559.
Ellis, T. M., Bowman, D. M. J. S. and Williamson, G. J. 2023. Ecoregion flammability thresholds: the global pyrogeography of dead fine fuel moisture content as a driver for wildfire activity. – University of Tasmania Research Data Portal, https://doi.org/10.25959/rbk3-5d65.
Fernandes, P. M., Botelho, H., Rego, F. and Loureiro, C. 2008. Using fuel and weather variables to predict the sustainability of surface fire spread in maritime pine stands. – Can. J. For. Res. 38: 190–201.
Field, R. D. 2020. Evaluation of global and fire weather and database reanalysis and and short-term forecast products. – Nat. Hazards Earth Syst. Sci. 20: 1123–1147.
Filkov, A., Duff, T. and Penman, T. 2019. Determining threshold conditions for extreme fire behaviour. Annual report 2018–2019. – Bushfire and Natural Hazards CRC.
Flannigan, M., Cantin, A. S., de Groot, W. J., Wotton, M., Newbery, A. and Gowman, L. M. 2013. Global wildland fire season severity in the 21st century. – For. Ecol. Manage. 294: 54–61.
Flannigan, M. D., Wotton, B. M., Marshall, G. A., de Groot, W. J., Johnston, J., Jurko, N. and Cantin, A. S. 2016. Fuel moisture sensitivity to temperature and precipitation: climate change implications. – Clim. Change 134: 59–71.
Furlaud, J. M., Prior, L. D., Williamson, G. J. and Bowman, D. M. 2021. Bioclimatic drivers of fire severity across the Australian geographical range of giant Eucalyptus forests. – J. Ecol. 109: 2514–2536.
Giglio, L., Descloitres, J., Justice, C. O. and Kaufman, Y. J. 2003. An enhanced contextual fire detection algorithm for MODIS. – Remote Sens. Environ. 87: 273–282.
Giglio, L., Boschetti, L., Roy, D. P., Humber, M. L. and Justice, C. O. 2018. The Collection 6 MODIS burned area mapping algorithm and product. – Remote Sens. Environ. 217: 72–85.
Hernandez, C., Drobinski, P. and Turquety, S. 2015. How much does weather control fire size and intensity in the Mediterranean region? – Ann. Geophys. 33: 931–939.
Hersbach, H. et al. 2020. The ERA5 global reanalysis. – Q. J. R. Meteorol. Soc. 146: 1999–2049.
Hessburg, P. F., Prichard, S. J., Hagmann, R. K., Povak, N. A. and Lake, F. K. 2021. Wildfire and climate change adaptation of western North American forests: a case for intentional management. – Ecol. Appl. 31: e02432.
Higuera, P. E. and Abatzoglou, J. T. 2020. Record-setting climate enabled the extraordinary 2020 fire season in the western United States. – Global Change Biol. 27: 1–2.
Jain, P., Castellanos-Acuna, D., Coogan, S. C., Abatzoglou, J. T. and Flannigan, M. D. 2022. Observed increases in extreme fire weather driven by atmospheric humidity and temperature. – Nat. Clim. Chang. 12: 63–70.
Jolly, W. M. and Johnson, D. M. 2018. Pyro-ecophysiology: shifting the paradigm of live wildland fuel research. – Fire 1: 8.
Jones, M. W., Abatzoglou, J. T., Veraverbeke, S., Andela, N., Lasslop, G., Forkel, M., Smith, A. J. P., Burton, C., Betts, R. A., van der Werf, G. R., Sitch, S., Canadell, J. G., Santín, C., Kolden, C., Doerr, S. H. and Le Quéré, C. 2022. Global and regional trends and drivers of fire under climate change. – Rev. Geophys. 60: e2020RG000726.
Keeley, J. E., Pausas, J. G., Rundel, P. W., Bond, W. J. and Bradstock, R. A. 2011. Fire as an evolutionary pressure shaping plant traits. – Trends Plant Sci. 16: 406–411.
Kelley, D. I., Bistinas, I., Whitley, R., Burton, C., Marthews, T. R. and Dong, N. 2019. How contemporary bioclimatic and human controls change global fire regimes. – Nat. Clim. Chang. 9: 690–696.
Krawchuk, M. A. and Moritz, M. A. 2011. Constraints on global fire activity vary across a resource gradient. – Ecology 92: 121–132.
Kruskal, W. H. and Wallis, W. A. 1952. Use of ranks in one-criterion variance analysis. – J. Am. Stat. Assoc. 47: 583–621.
Lavers, D. A., Simmons, A., Vamborg, F. and Rodwell, M. J. 2022. An evaluation of ERA5 precipitation for climate monitoring. – Q. J. R. Meteorol. Soc. 148: 3152–3165.
Le Page, Y., Oom, D., Silva, J. M. N., Jönsson, P. and Pereira, J. M. C. 2010. Seasonality of vegetation fires as modified by human action: observing the deviation from eco-climatic fire regimes. – Global Ecol. Biogeogr. 19: 575–588.
Little, J. K., Prior, L. D., Williamson, G. J., Williams, S. E. and Bowman, D. M. 2012. Fire weather risk differs across rain for-

est–savanna boundaries in the humid tropics of north-eastern Australia. – Austral Ecol. 37: 915–925.
Luke, R. H. and McArthur, A. G. 1978. Bushfires in Australia. – Australian Government Publishing Service.
Mariani, M., Connor, S. E., Theuerkauf, M., Herbert, A., Kuneš, P., Bowman, D., Fletcher, M.-S., Head, L., Kershaw, A. P., Haberle, S. G., Stevenson, J., Adeleye, M., Cadd, H., Hopf, F. and Briles, C. 2022. Disruption of cultural burning promotes shrub encroachment and unprecedented wildfires. – Front. Ecol. Environ. 20: 292–300.
McColl-Gausden, S. C., Bennett, L. T., Clarke, H. G., Ababei, D. A. and Penman, T. D. 2022. The fuel–climate–fire conundrum: how will fire regimes change in temperate eucalypt forests under climate change? – Global Change Biol. 28: 5211–5226.
McElhinny, M., Beckers, J. F., Hanes, C., Flannigan, M. and Jain, P. 2020. A high-resolution reanalysis of global fire weather from 1979 to 2018 – overwintering the drought code. – Earth Syst. Sci. Data 12: 1823–1833.
Murphy, B. P., Bradstock, R. A., Boer, M. M., Carter, J., Cary, G. J., Cochrane, M. A., Fensham, R. J., Russell-Smith, J., Williamson, G. J. and Bowman, D. M. J. S. 2013. Fire regimes of Australia: a pyrogeographic model system. – J. Biogeogr. 40: 1048–1058.
Mutch, R. W. 1970. Wildland fires and ecosystems – a hypothesis. Ecology 51: 1046–1051.
Nolan, R. H., Boer, M. M., de Dios, V. R., Caccamo, G. and Bradstock, R. A. 2016. Large-scale, dynamic transformations in fuel moisture drive wildfire activity across southeastern Australia. – Geophys. Res. Lett. 43: 4229–4238.
Nolan, R. H., Boer, M. M., Collins, L., de Dios, V. R., Clarke, H., Jenkins, M., Kenny, B. and Bradstock, R. A. 2020. Causes and consequences of eastern Australia's 2019–20 season of megafires. – Global Change Biol. 26: 1039–1041.
Olson, D. M., Dinerstein, E., Wikramanayake, E. D., Burgess, N. D., Powell, G. V. N., Underwood, E. C., D'Amico, J. A., Itoua, I., Strand, H. E., Morrison, J. C., Loucks, C. J., Allnutt, T. F., Ricketts, T. H., Kura, Y., Lamoreux, J. F., Wettengel, W. W., Hedao, P. and Kassem, K. R. 2001. Terrestrial ecoregions of the world: a new map of life on earth. BioScience 51: 933–938.
Olson, J. S. 1963. Energy storage and the balance of producers and decomposers in ecological systems. – Ecology 44: 322–331.
Pausas, J. G. and Bradstock, R. A. 2007. Fire persistence traits of plants along a productivity and disturbance gradient in Mediterranean shrublands of south-east Australia. – Global Ecol. Biogeogr. 16: 330–340.
Pausas, J. G. and Keeley, J. E. 2009. A burning story: the role of fire in the history of life. – BioScience 59: 593–601.
Pausas, J. G. and Paula, S. 2012. Fuel shapes the fire–climate relationship: evidence from Mediterranean ecosystems. – Global Ecol. Biogeogr. 21: 1074–1082.
Pausas, J. G. and Ribeiro, E. 2013. The global fire–productivity relationship. – Global Ecol. Biogeogr. 22: 728–736.
Pausas, J. G. and Bond, W. J. 2020. Alternative biome states in terrestrial ecosystems. – Trends Plant Sci. 25: 250–263.
Pausas, J. G. and Keeley, J. E. 2021. Wildfires and global change. – Front. Ecol. Environ. 19: 387–395.
Running, S., Mu, Q. and Zhao, M. 2015. MOD17A3 MODIS/Terra gross primary productivity yearly L4 global 1km SIN grid. – NASA EOSDIS Land Processes Distributed Active Archive Center.
Schunk, C., Wastl, C., Leuchner, M. and Menzel, A. 2017. Fine fuel moisture for site- and species-specific fire danger assessment in comparison to fire danger indices. – Agric. For. Meteorol. 234–235: 31–47.
Scott, A. C. and Glasspool, I. J. 2006. The diversification of Paleozoic fire systems and fluctuations in atmospheric oxygen concentration. – Proc. Natl Acad. Sci. USA 103: 10861–10865.
Senande-Rivera, M., Insua-Costa, D. and Miguez-Macho, G. 2022. Spatial and temporal expansion of global wildland fire activity in response to climate change. – Nat. Commun. 13: 1208.
Sharples, J. J., Cary, G. J., Fox-Hughes, P., Mooney, S., Evans, J. P., Fletcher, M.-S., Fromm, M., Grierson, P. F., McRae, R. and Baker, P. 2016. Natural hazards in Australia: extreme bushfire. – Clim. Change 139: 85–99.
Slijepcevic, A., Anderson, W. R., Matthews, S. and Anderson, D. H. 2015. Evaluating models to predict daily fine fuel moisture content in eucalypt forest. – For. Ecol. Manage. 335: 261–269.
van Oldenborgh, G. J., Krikken, F., Lewis, S., Leach, N. J., Lehner, F., Saunders, K. R., van Weele, M., Haustein, K., Li, S., Wallom, D., Sparrow, S., Arrighi, J., Singh, R. K., van Aalst, M. K., Philip, S. Y., Vautard, R. and Otto, F. E. L. 2021. Attribution of the Australian bushfire risk to anthropogenic climate change. – Nat. Hazards Earth Syst.Sci. 21: 941–960.
van Wagner, C. E. 1987. Development and structure of the Canadian forest fire weather index system. Forestry Tech. Rep. 35. – Canadian Forest Service, Petawawa National Forestry Institution.
Varner, J. M., Kane, J. M., Kreye, J. K. and Engber, E. 2015. The flammability of forest and woodland litter: a synthesis. – Curr. For. Rep. 1: 91–99.
Westerling, A. L. 2016. Increasing western US forest wildfire activity: sensitivity to changes in the timing of spring. – Phil. Trans. R. Soc. B 371: 20150178.
Williams, A. P., Abatzoglou, J. T., Gershunov, A., Guzman-Morales, J., Bishop, D. A., Balch, J. K. and Lettenmaier, D. P. 2019. Observed impacts of anthropogenic climate change on wildfire in California. – Earth's Future 7: 892–910.
Williamson, G. J., Prior, L. D., Jolly, W. M., Cochrane, M. A., Murphy, B. P. and Bowman, D. M. 2016. Measurement of inter- and intra-annual variability of landscape fire activity at a continental scale: the Australian case. – Environ. Res. Lett. 11: 035003.
Wotton, B. M. 2008. Interpreting and using outputs from the Canadian forest fire danger rating system in research applications. – Environ. Ecol. Stat. 16: 107–131.
Wotton, B. M. and Beverly, J. L. 2007. Stand-specific litter moisture content calibrations for the Canadian fine fuel moisture code. – Int. J. Wildland Fire 16: 463.
Wotton, B. M., Flannigan, M. D. and Marshall, G. A. 2017. Potential climate change impacts on fire intensity and key wildfire suppression thresholds in Canada. – Environ. Res. Lett. 12: 095003.
Wouters, H., Berckmans, J., Maes, R., Vanuytrecht, E. and Ridder, K. D. 2021. Global bioclimatic indicators from 1979 to 2018 derived from reanalysis. – European Centre for Medium-Range Weather Forecasts.
Wyse, S. V., Perry, G. L. W., O'Connell, D. M., Holland, P. S., Wright, M. J., Hosted, C. L., Whitelock, S. L., Geary, I. J., Maurin, K. J. L. and Curran, T. J. 2016. A quantitative assessment of shoot flammability for 60 tree and shrub species supports rankings based on expert opinion. – Int. J. Wildland Fire 25: 466–477.